CDF note xxxx

Search for Pentaquark states decaying to $\mathbf{D^{(*)}\bar{p}}$

The CDF Collaboration
URL http://www-cdf.fnal.gov

(Dated: October 20, 2004)

The long-standing question of whether there are 5-quark baryons has been reinvigorated in the past year by multiple reports of the existence of a baryon decaying to a KN final state with positive strangeness. This state, the $\Theta(1540)$, is manifestly exotic and had been predicted in 1997 as the lightest member of an anti-decuplet of states on the basis of a chiral soliton model by Diakonov, Petrov, and Polyakov [1]. There should be a charmed analog of this decuplet. Charmed pentaquarks had been predicted much earlier by other authors based on different models. The H1 experiment recently reported the observation of a narrow baryon at 3099 MeV/c^2 decaying to D^*p + c.c. [8] This state is a candidate for the charmed pentaquark Θ_c or perhaps an excited state thereof. search for this state at CDF detector using data taken with displaced track trigger. No signal was found. This note is the continuation of our studies, it describes a comprehensive search for pentaquarks states decaying to $D^{(*)}\bar{p}$

Preliminary Results for Summer 2004 Conferences

I. INTRODUCTION

Searches for states, characterized by so-called exotic quantum numbers, i.e., quantum numbers that cannot be obtained from minimal $(q\bar{q})$ or (qqq) configurations of standard mesons and baryons, have taken place since the introduction of QCD and quark model. Until recently, these searches yielded very little conclusive evidence for such states.

During 2003, however, the situation has changed dramatically. An observation of a narrow resonance at (1540 ± 10) MeV/c^2, called Θ^+, decaying to nK^+, produced in $\gamma n \to K^-\Theta^+$, was reported by LEPS [5]. The state has exotic quantum number, positive strangeness, and cannot exist in a simple three-quark model. A pentaquark interpretation was employed suggesting the quark content to be $(uudd\bar{s})$. This observation was confirmed by various experiments using incident beams of real and quasi-real photons, kaons and neutrinos [6].

From the QCD standpoint the mutliquark configurations are allowed as long as they form color singlet states. These states were proposed in the context of constituent quark models [2], quark models with correlated quarks [3, 4] and in chiral soliton model [1]. Most recently Diakonov, Petrov and Polyakov predicted the mass and the width of the Θ^+ to be 1540 GeV/c^2 and 15 MeV/c^2 respectively [1].

Afterwords, followed two other manifestly exotic S=-2 baryon states decaying to $\Xi^-\pi^\pm$ observed in pp collisions of CERN SPS at $\sqrt{s} = 17.2$ GeV by NA49 [7]. The particle was dubbed the Φ. The combined mass of Φ^{--} and Φ^0 was measured to be (1.862 ± 0.002) GeV/c^2. These resonances were interpreted as $I_3 = -3/2$ and $I_3 = +1/2$ partners of isospin quadruplet of five-quark states with quark contents $(dsds\bar{u})$ and $(dsus\bar{d})$ respectively.

The Θ^+ and $\Xi^{--,0}$ states are consistent with being members of minimal SU(3) anti-decuplet of pentaquark states predicted in the chiral soliton model of baryons[1].

In March 2004, the H1 experiment at HERA reported a narrow resonance, the Θ_c, decaying to $D^{*-}p$ at a mass 3.099 GeV/c^2 [8]. It can be seen as the charmed analog of Θ^+ with quark content $(uudd\bar{c})$.

For strongly decaying particles all reported states are unusually narrow with widths consistent with detector resolution. The reported masses of Θ^+ vary widely over a range, between 1526 and 1542 MeV/c^2, for different experiments.

All pentaquark observations are based on relatively small data samples. Typically $20 - 100$ signal events are seen with a significance in the range from 4 to 6σ. While the Θ^+ has been seen by several experiments, an independent confirmation of the $\Xi^{--,0}_{3/2}$ and Θ_c states has not been made. Definitely high statistics experiments are needed to establish pentaquark states unambiguously.

Pentaquark states, if exist, would give rise to a rich spectrum of decays of the type MESON + BARYON(ANTI-BARYON). We considered pentaquarks that would strongly decay to D-mesons and anti-proton. These decay modes are especially attractive as two tracks from displaced D vertex come in on unique CDF B-hadronic trigger. In the H1 pentaquark paper they mentioned that the fraction of Θ_c^0 is roughly 1% of the total D^* production [8]. Assuming that the dominant production mechanism of Θ_c^0 in deep inelastic ep collisions is fragmentation of the c-quark produced in $\gamma^* p \to c\bar{c}$, the fragmentation probability $f(\bar{c} \to \Theta_c^0)$ could be 2.35×10^{-3}. If this was true then CDF should see $\sim 10^4$ per 100 pb^{-1} [9].

In this note we describe the results of comprehensive searches for charmed pentaquarks in the decay modes $D^{*-}p$, D^-p, $\bar{D}^0p$ and D^0p produced in $p\bar{p}$ collisions at $\sqrt{s} = 1.96$ TeV.

The CDF detector is described in detail in [10].

II. DATA SAMPLE & EVENT SELECTION

This analysis is based on an integrated luminosity of 240 pb^{-1} collected with the CDFII detector between March 2002 and January 2004. The CDF II detector has a three level trigger system. The data used in this analysis were obtained by a trigger that was specialized for recording hadronic b-decays and c-decays. This trigger used data from the COT and the custom hardware track trigger processor (XFT) to identify charged tracks at Level 1 of the trigger. Events with two oppositely charged tracks were accepted by the Level 1 trigger if each track had $p_T > 2.0$ GeV/c, the scalar sum of the two transverse momenta exceeded 5.5 Gev/c and the angular difference between the tracks was less than 135^o. Level 2 of the CDF trigger combines data from different detector subsystems. At this level, data from the SVXII detector is used in the Silicon Vertex Trigger system to improve the track measurement, and require the track impact parameter with respect to the beam (d_0) to fall within the range $120\mu m < |d_0| < 1mm$.

A. Reference channels

The production mechanism of pentaquark states in $p\bar{p}$ collisions is unknown. The evidence for the Θ_c production in Deep Inelastic scattering reported by the H1 Collaboration may suggest a production via c-quark fragmentation. On the other hand, the pentaquark states may be produced in the decays of b-hadrons. Both types of events are efficiently triggered by displace track trigger due to displaced tracks from D^- or $\bar{D}^0$ decays. In the case of pentaquark production from b-hadrons, the proton could be a trigger track. Figure 1 shows two distinct vertex configurations.

As reference channels we use well established decay modes of $D^{**} \to D^{(*)}\pi$. We expect huge statistics of D^{**}, hence the optimization of common cuts, the cuts that are not defined by specific decay kinematics, was performed using clear D^{**} signals. The optimal cuts are summarized in Table I.

Cut	D^{**}	D^*	D^+	D^0
ΔM		± 1.8 MeV/c^2	± 20 MeV/c^2	± 20 MeV/c^2
`CTVMFT` prob	$> 0.1\%$	$> 0.1\%$	$> 0.1\%$	$> 0.1\%$
L_{xy}			> 0.08 cm	> 0.06 cm
$L_{xy}/\sigma(L_{xy})$			> 6	> 3
$\lvert d_0 \rvert$			< 0.008 cm	< 0.008 cm

TABLE I: List of cuts applied to reference modes and carried over to promptly produced pentaquark modes.

An invariant mass spectrum of $D^+\pi^-$ is shown in Figure 2. A prominent peak corresponding to decay $D_2^{*0} \to D^+\pi^-$ is clearly visible at the mass about 2.46 GeV/c^2. There is also a satellite lower mass bump due to $D^{*0} \to D^{*+}\pi^-$ decays with $D^{*+} \to D^+\pi^0(\gamma)$. The D^+ from D^{*+} decay combines with π^- from D^{**} decay and due to extremely low Q-value in the decay $D^{*+} \to D^+\pi^0(\gamma)$ produces a clear bump, which in fact is a superposition of two bumps, corresponding to reflections from $D_1^0(2420)$ and $D_2^{*0}(2460)$. The spectrum shown in Figure 2 is fit with the function:

$$\begin{aligned}\mathcal{F} = \; & dm^b \cdot \left(\sum_{i=0}^{3} a_i \cdot dm^i\right) + N_0 \cdot BW \otimes NGauss(m, \sigma_0, m_0, \Gamma) + \\ & N_1 \cdot Gauss(m, \sigma_1, m_1) + N_2 \cdot Gauss(m, \sigma_2, m_2),\end{aligned} \quad (1)$$

where

- $dm = m - (m_\pi + m_D)$
- $Gauss(m, \sigma_1, m_1)$ and $Gauss(m, \sigma_2, m_2)$ describe feed-down peaks
- $BW \otimes Gauss(m, \sigma_0, m_0, \Gamma)$ describes signal peak, the BW denotes non-relativistic Breit-Wigner resonance form.

All parameters were set free except the mass resolution of the D_2^{*0} peak, which is known to be 7.7 MeV/c^2 . The fit yielded relevant parameter values broken down in Table II.

An invariant mass spectrum of $D^0\pi^+$ is shown in Figure 3. The picture is dominated by a huge signal from $D^{*+} \to D^0\pi$ decays. Also two higher mass peaks are visible. The higher mass one corresponds to decays $D_2^{*0} \to D^0\pi^+$ the lower mass satellite peak is attributed to decays $D^{*+} \to D^{*0}\pi^+$ followed by $D^{*0} \to D^0\pi^0(\gamma)$. The D^0 from D^{*0} decay combines with π^+ from D^{**} decay and due to extremely low Q-value in the decay $D^{*0} \to D^0\pi^0(\gamma)$ produces a clear bump, which in fact is a superposition of two bumps, corresponding to reflections from $D_1^0(2420)$ and $D_2^{*0}(2460)$. The spectrum shown in Figure 3 is fit with the same function (1) after substituting appropriate threshold mass. The D^* peak region was not included into the fit. The fit results are summarized in Table III.

A mass difference spectrum $M(D^{*+}\pi^-) = M(D^{*+}\pi^-) - M(D^{*+}) + 2.01$ is shown in Figure 4. In this case we have two overlapping narrow states - D_1^0 and D_2^{*0}. The function (1) has been modified to include second Breit-Wigner convoluted with Gaussian resolution function. The fit results are summarized in Table IV.

III. $D^{*-,-,0}p$ SELECTION

The selection of $D^{*-,-,0}p$ candidates is identical to the selection of corresponding reference modes discussed in the previous subsection, except that the proton mass is used for the fourth track.

Parameter	value	Unit
N_0	31726 ± 1338	
σ_0	7.7(fixed)	MeV/c^2
Γ	42.3 ± 2.2	MeV/c^2
m_0	2468.1 ± 0.6	MeV/c^2
N_1	2719 ± 1175	
σ_1	12.3 ± 2.1	MeV/c^2
m_1	2279.5 ± 3.3	MeV/c^2
N_2	3895 ± 1330	
σ_2	20.2 ± 5.1	MeV/c^2
m_2	2310.3 ± 7.4	MeV/c^2

TABLE II: Parameters of binned fit to $M(D^+\pi^-)$ spectrum.

Parameter	value	Unit
N_0	15340 ± 1573	
σ_0	7.7(fixed)	MeV/c^2
Γ	39.8 ± 5.0	MeV/c^2
m_0	2468.8 ± 1.4	MeV/c^2
N_1	5787 ± 1834	
σ_1	11.6 ± 2.3	MeV/c^2
m_1	2277.5 ± 1.9	MeV/c^2
N_2	12009 ± 1895	
σ_2	25.6 ± 2.4	MeV/c^2
m_2	2309.0 ± 5.0	MeV/c^2

TABLE III: Parameters of binned fit to $M(D^0\pi^+)$ spectrum.

A. Proton Identification

Particle identification for the proton tracks is a crucial piece of the analysis. Because the predicted range of proton momenta starts near 1 GeV/c and goes above 8 GeV/c, according to simulation, we must use both time of flight (TOF) and dE/dx techniques.

B. Combining ToF and dE/dx information

The ToF and dE/dx measurements are *independent* allowing one to make a combined χ^2 for PID:

$$\chi_i^2 = \chi_{\mathrm{i}}^2(\mathrm{ToF}) + \chi_{\mathrm{i}}^2(\mathrm{dE/dx})(\mathrm{COT}) \tag{2}$$

where

$$\chi_i^2(ToF) = \left(\frac{ToF(mes) - ToF(exp)_i}{\sigma_{ToF}}\right)^2 \tag{3}$$

Parameter	value	Unit
$N(D_2^{*0})$	6247 ± 1711	
σ_0	3.8 (fixed)	MeV/c^2
Γ	67.1 ± 0.012	MeV/c^2
Mass(D_2^{*0})	2457.7 ± 0.5	MeV/c^2
$N(D_1^0)$	3724 ± 899	
σ_1	3.8 (fixed)	MeV/c^2
$M(D_1^0)$	2423.3 ± 1.5	MeV/c^2

TABLE IV: Parameters of binned fit to $M(D^{*+}\pi^-)$ spectrum.

$$\chi_i^2(dE/dx) = \left(\frac{dE/dx(mes) - dE/dx(exp)_i}{\sigma_{dE/dx}}\right)^2 \tag{4}$$

where $\mathrm{i} = \mathrm{p}, \mathrm{K}, \pi, \mathrm{e}, \mu$. We then calculate a likelihood for each particle hypothesis:

$$\mathrm{lh(i)} = \exp(-\chi_\mathrm{i}^2/2) \tag{5}$$

and combine them into likelihood ratio:

$$\mathrm{LH_i} = \frac{\mathrm{lh(i)}}{\mathrm{lh(p) + lh(K) + lh(e)} + \mathrm{lh}(\mu) + \mathrm{lh}(\pi)}. \tag{6}$$

We considered $\Lambda_\mathrm{c} \to \mathrm{pK}^-\pi^+$ decays produced in association with muons in b-hadronic sample as proton source to test particle identification cut.

The resulting invariant mass spectrum of $\mathrm{pK}^-\pi^+$ combinations is presented in Figure 5a). The distribution was fit with the sum of Gaussian signal and linear background. All parameters of the fit function were allowed to float. There are 2511 ± 123 in Λ_c events in the peak at the mass of (2285.4 ± 0.4) MeV/c^2 with the mass resolution of (7.8 ± 0.4) MeV/c^2. The fit quality is $\chi^2/\mathrm{ndf} = 35.5/35$ translating into probability of 0.45.

We studied the behavior of Λ_c signal significance defined as $\frac{S}{\sqrt{S+B}}$ using sideband subtraction as the function of $\mathrm{LH_p(p)}$ cut in eight $\mathrm{p_T(p)}$ bins. The signal region was defined as:

$$|\mathrm{M(pK}\pi) - \mathrm{M}(\Lambda_\mathrm{c})| < 21\ \mathrm{MeV/c^2}$$

and sideband region was defined as

$$28 < |\mathrm{M(pK}\pi) - \mathrm{M}(\Lambda_\mathrm{c})| < 49\ \mathrm{MeV/c^2}.$$

The background events were taken from $\mathrm{D^*p}$ sample. The candidates having an invariant mass outside the pentaquark search window were used. The optimum is reached at $\mathrm{LH_p(p)} > 0.3$, the efficiency for the signal is 73%, while background is reduced by more than a factor of 5. The Figure 5 b) shows $\mathrm{pK}\pi$ invariant mass spectra with $\mathrm{LH_p(p)} > 0.3$. The mass spectrum was fit with the sum of Gaussian and linear background. An excellent signal of 1810 ± 63 events is present at the mass (2285.7 ± 0.3) MeV/c^2. The fit quality is $\chi^2/\mathrm{ndf} = 44.4/35$, fit probability 0.13. Signal improvement is evident.

To choose proton ID cut for pentaquark searches we rely on optimization results obtained using different score function, $\frac{S}{1.35+\sqrt{B}}$, which is more appropriate for searches. The optimal cut turned out to be higher, $\mathrm{LH_p(p)} > 0.4$, as expected.

C. $\mathrm{D}^{*-,-,0}\mathrm{p}$ spectra with proton PID

Having determined an optimal proton PID cut we applied it to our $\mathrm{D^{*-}p}$, $\mathrm{D^-p}$ and $\mathrm{D^0p}$ candidates. No signals were found and we extracted 90% Confidence Level limits on event yields as the function of mass. The mass spectra and yields vs mass plots for each mode are presented in Figures 6–Figure 9.

The upper limits obtained in the search window (3.099 ± 0.0174) are summarized in Table V

	Event yield @ 90% CL	
Mode	$\Gamma = 0$ MeV/c^2	$\Gamma = 12$ MeV/c^2
$\mathrm{D^{*-}p}$	21	32
$\mathrm{D^-p}$	80	84
$\bar{\mathrm{D}}^0\mathrm{p}$	87	122
$\mathrm{D^0p}$	97	245

TABLE V: Upper limits on pentaquark event yields.

IV. CONCLUSION

Using a high statistics charm sample collected with the displaced track trigger we searched for the exotic baryons decaying to $D^{*-}p$, $D^{-}p$, $D^{0}p$ and $\bar{D}^{0}p$. No narrow resonances were found in either mode. We utilized particle identification capabilities of the CDF detector and applied combined TOF and dE/dx PID cut to proton candidates. The cut was optimized on independent calibration sample of $\Lambda_c \to pK\pi$ decays. The PID cut did not help reveal narrow structures in invariant mass spectra studied. We reported upper limits in on event yield in each channel.

[1] Diakonov, Petrov, and Polyakov, Z. Physik A **359**, 308 (1997).
[2] D. Strottman, Phys. Rev. D **20**, 748 (1979).
[3] R. L. Jaffe and F. Wilczek, Phys. Rev. Lett. **91**, 232003 (2003) [arXiv:hep-ph/0307341].
[4] M. Karliner and H. J. Lipkin, Phys. Lett. B **575**, 249 (2003) [arXiv:hep-ph/0402260].
[5] T. Nakano *et al.*, Phys. Rev. Lett. **91**, 01200
[6] V. V. Barmin *et al.*, Phys. Atom. Nucl. **66**, 1715; J. Barth *et al.* Phys. Lett. B **572** 127; A. E. Asratyan *et al.*, Phys. Atom. Nucl. **67**, 682; V. Kubarovsky *et al.*, Phys. Rev. Lett. **92**, 032001; A. Airapetian *et al.*, Phys. Lett. B **587** 213
[7] C. Alt *et al.*, Phys. Rev. Lett. **92**, 042003
[8] A. Aktas *et al.*, hep-ex/0403017
[9] K. Cheung, arXiv:hep-ph/0405281
[10] F. Abe, et al., Nucl. Instrum. Methods Phys. Res. A **271**,
[11] T. Yamashita *et al.*, "Measurement of the Run-II Inclusive J/Psi Cross-section" CDF/PHYS/BOTTOM/CDFR/6288
[12] Particle Data Group, K. Hagiwara *et al.*, Phys. Rev. **D 66**, 2002

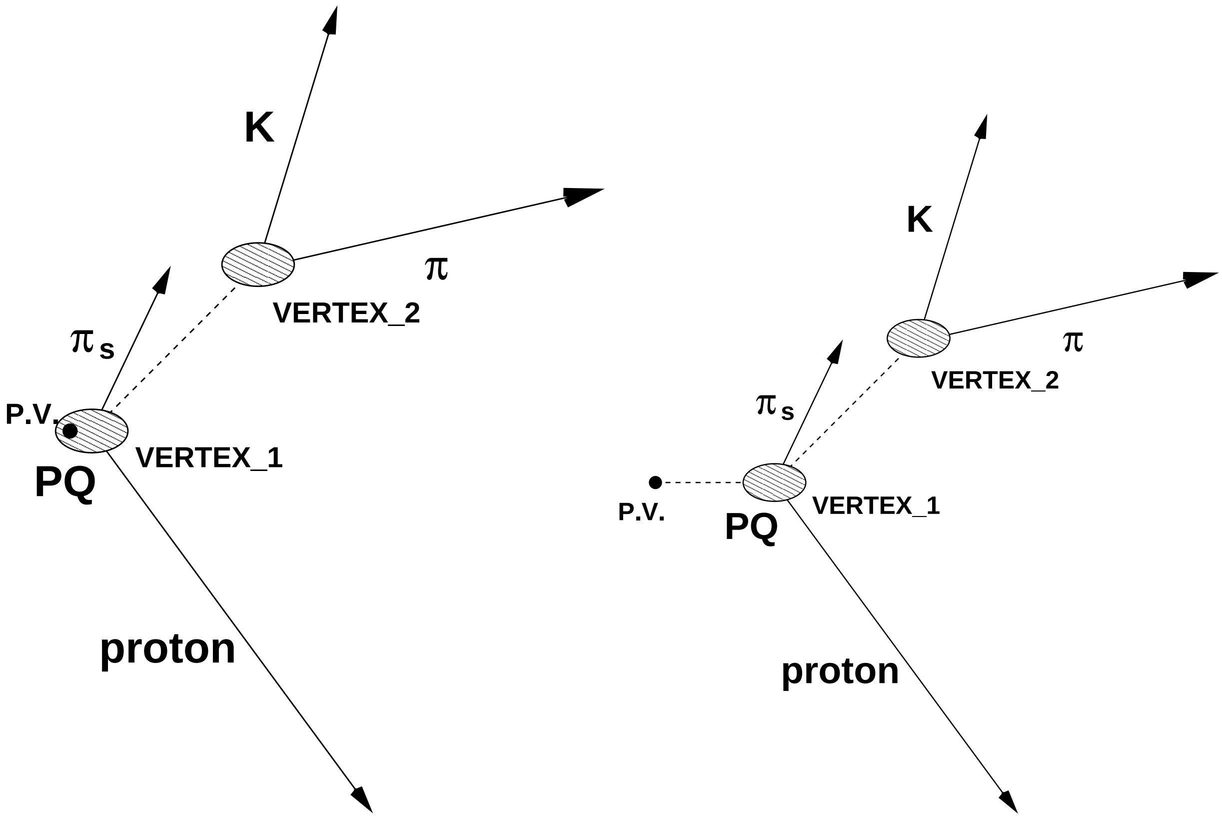

FIG. 1: Two classes of events corresponding to different pentaquark production mechanisms. Prompt production from charm quark fragmentation (left figure), production in decays of b-hadrons (right figure).

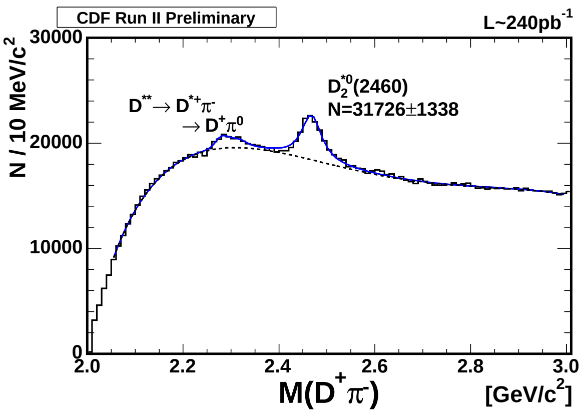

FIG. 2: An invariant mass of $D^+\pi^-$ combinations

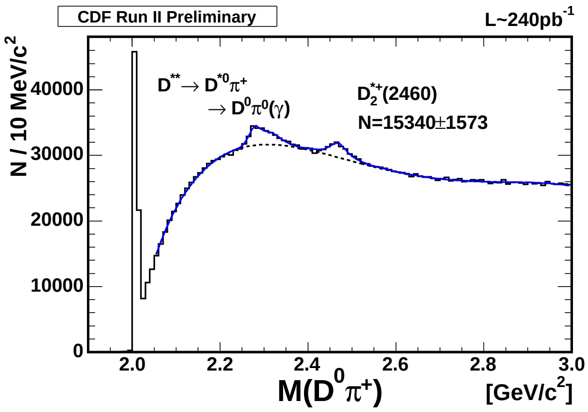

FIG. 3: An invariant mass of $D^0\pi^+$ combinations

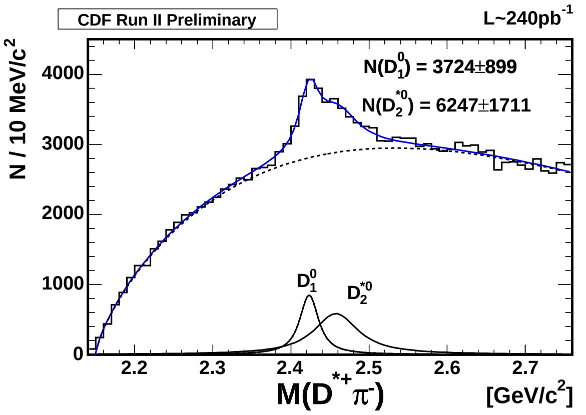

FIG. 4: A D^{**} mass difference $(\Delta M + M_{D^{*+}})$ spectrum.

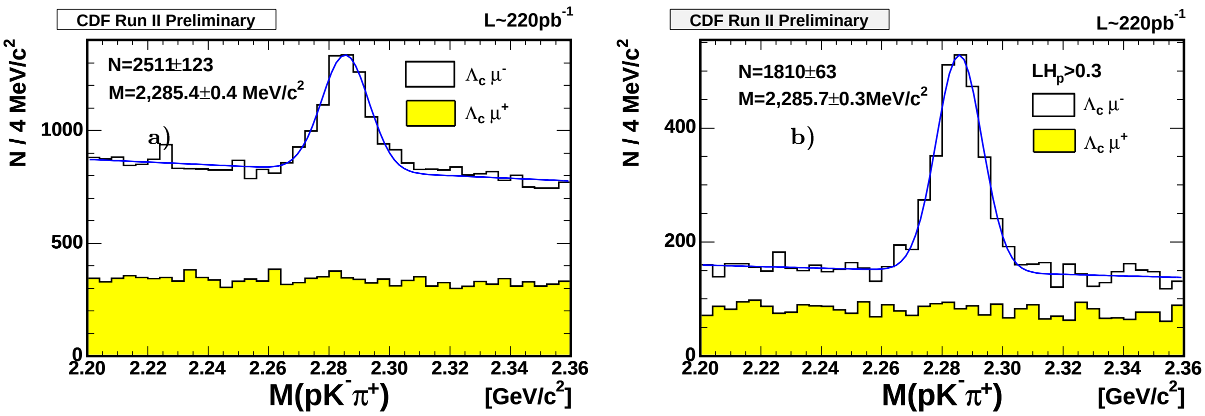

FIG. 5: $pK\pi$ invariant mass spectra a) without PID cut, $LH_p(p) > 0.3$ cut (b).

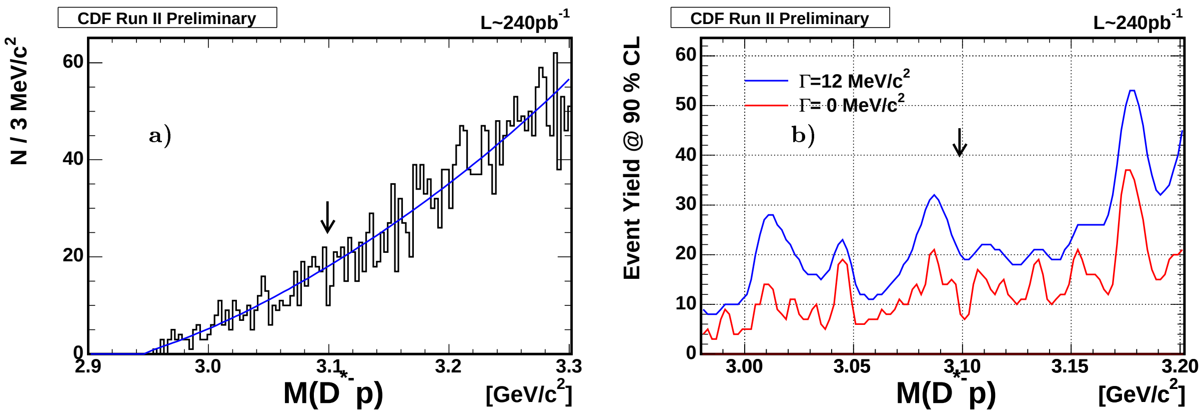

FIG. 6: a) ($D^{*+}\bar{p}$) mass difference spectra ($\Delta M + M_{D^{*+}}$) with $LH_p > 0.4$ cut applied to decay proton. The smooth curves represent the results of unbinned log-likelihood fits described in the text; b) 90% upper limit on event yield vs mass.

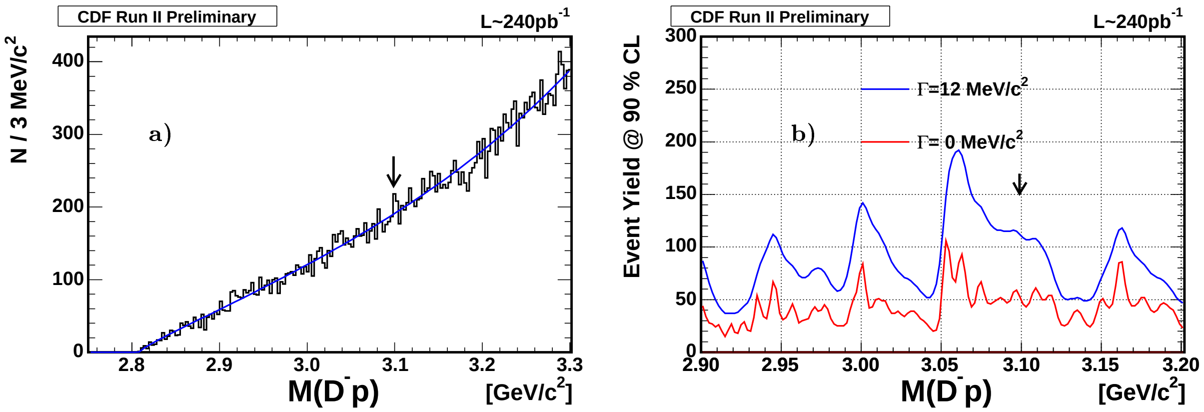

FIG. 7: a) (D^-p) mass spectra with $LH_p > 0.4$ cut applied to decay proton. The smooth curves represent the results of unbinned log-likelihood fits described in the text; b) 90% upper limit on event yield vs mass.

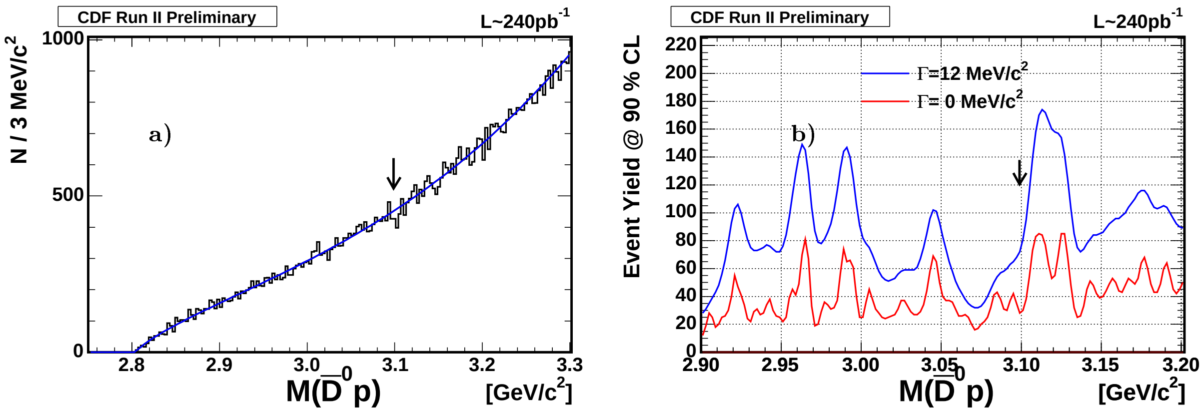

FIG. 8: a) ($\bar{D}^0p$) mass with $LH_p > 0.4$ cut applied to decay proton. The smooth curves represent the results of unbinned log-likelihood fits described in the text; b) 90% upper limit on event yield vs mass.

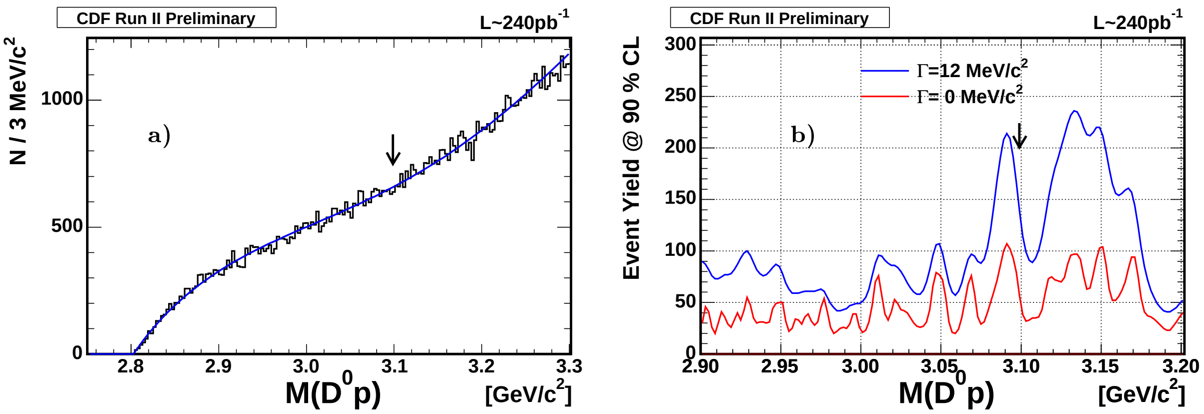

FIG. 9: a) (D^0p) mass with $LH_p > 0.4$ cut applied to decay proton. The smooth curves represent the results of unbinned log-likelihood fits described in the text; b) 90% upper limit on event yield vs mass.